Polarization-Sensitive NALM for Two-Level Amplitude Regeneration

Olivier Pottiez, I. Armas-Rivera, Y. E. Bracamontes-Rodriguez, G. Beltran-Perez, M. Duran-Sanchez, R. I. Alvarez-Tamayo, B. Ibarra-Escamilla, and E. A. Kuzin

***Abstract*— We propose and study analytically and numerically a nonlinear amplifying loop mirror scheme for multilevel amplitude regeneration, whose operation relies on the manipulation of light polarization. Polarization control increases the number of degrees of freedom of the setup, making it easier to meet the demanding requirements for regenerating complex modulation formats. By adjusting one of those additional parameters, namely, the ellipticity of input polarization, if all the other ones are properly set and fixed, the transfer characteristic is shaped for optimal two-level amplitude regeneration for two different state power ratios. The cascadability of the proposed scheme is demonstrated for the optical star-8 quadrature amplitude modulation format as an example.**

***Index Terms*— All-optical regeneration, nonlinear amplifying loop mirror (NALM), optical polarization control, quadrature amplitude modulation (QAM).**

I. Introduction

TAKING advantage of the ultrafast response time of the optical Kerr effect in fiber, the Nonlinear Optical Loop Mirror (NOLM) [1] and Nonlinear Amplifying Loop Mirror (NALM) [2] have long been considered for all-optical processing tasks, in particular regeneration [3], [4]. Recently, the increasing capacity demand has led to the emergence of complex modulation formats [5], triggering the quest for advanced all-optical regeneration solutions. Regeneration of constellations involving multiple amplitude and phase states is a challenging task involving phase-preserving [6] multilevel amplitude regeneration, in addition to phase regeneration [7]. Due to the periodicity of their transmission, NOLMs and NALMs appear naturally adapted for multilevel regeneration. Although solutions for simultaneous multilevel amplitude and phase regeneration are under development [8], another strategy consists in focusing on phase-preserving amplitude regeneration, as amplitude noise reduction not only restores the separation between adjacent power states but also reduces the major source of phase noise, which arises from nonlinear amplitude-to-phase noise conversion [6], [9]. Alternatively, the use of amplitude regenerators in combination with phase regenerators is being considered [10].

In [10], a simple NOLM-based scheme for multilevel (9 or more) amplitude regeneration has been proposed. In general however, NOLM- or NALM-based amplitude regeneration schemes are limited to two levels [8], [9], with non-optimal amplitude regeneration of at least one of the two states. This is because the slopes of the plateau regions in the power transfer characteristic do not cancel out for the same adjustments of parameters. This is an issue, in particular for cascaded configurations, as it was shown that regenerative performances degrade for imperfectly flat plateaus [11]. Another aspect to take into account for cascading regenerators, is that the state power ratio must be conserved through each regenerator. Hence, the multiple constraints on the transfer characteristic for proper multilevel amplitude regeneration exert a strong pressure on the existing adjustment parameters, which will be relaxed if new parameters are introduced.

The emergence of advanced constellations implies that not only the intensity, but also the phase of the optical signal is controlled and manipulated. Besides, three-dimensional constellations, with the additional inclusion of polarization states, are also being explored [12]. In contrast, light polarization is an aspect that is commonly passed over in most NOLM or NALM devices. In previous works by our group [13]–[16], polarization control was implemented in a NOLM scheme in order to improve its flexibility, and was applied to the regeneration of binary signals [17]. In this letter we propose a NALM for two-level amplitude regeneration, whose transmission can be adjusted through polarization adjustments. It will be referred to in the following as the P-NALM.

II. Device Description and Principle

The P-NALM scheme is shown in Fig. 1. The loop includes a length L of zero-dispersion, highly nonlinear fiber (HNLF) with nonlinear coefficient γ (for linearly polarized light). As in [6], the device is power-asymmetric due to the use of both an asymmetric *C:(1-C)* coupler and a bidirectional

Manuscript received May 8, 2015; revised July 6, 2015; accepted July 24, 2015. Date of publication July 28, 2015; date of current version September 23, 2015. This work was supported by the Consejo Nacional de Ciencia y Tecnología under Grant 130966.

O. Pottiez is with the Centro de Investigaciones en Óptica, León 37150, Mexico (e-mail: pottiez@cio.mx).

I. Armas-Rivera, Y. E. Bracamontes-Rodriguez, and G. Beltran-Perez are with the Facultad de Ciencias Físico-Matemáticas, Benemérita Universidad Autónoma de Puebla, Pue 72000, Mexico (e-mail: ivan_rr1@hotmail.com; yazmin_1985@yahoo.com.mx; gbeltran@fcfm.buap.mx).

M. Duran-Sanchez is with the Instituto Nacional de Astrofísica, Óptica y Electrónica, Puebla 72824, Mexico, and also with the Consejo Nacional de Ciencia y Tecnología, México D.F. 39040, Mexico (e-mail: maratonista@hotmail.com).

R. I. Alvarez-Tamayo, B. Ibarra-Escamilla, and E. A. Kuzin are with the Instituto Nacional de Astrofísica, Óptica y Electrónica, Puebla 72824, Mexico (e-mail: mduransa@conacyt.mx; baldemar@inaoep.mx; ekuz@inaoep.mx).

Color versions of one or more of the figures in this letter are available online at http://ieeexplore.ieee.org.

Digital Object Identifier 10.1109/LPT.2015.2461459

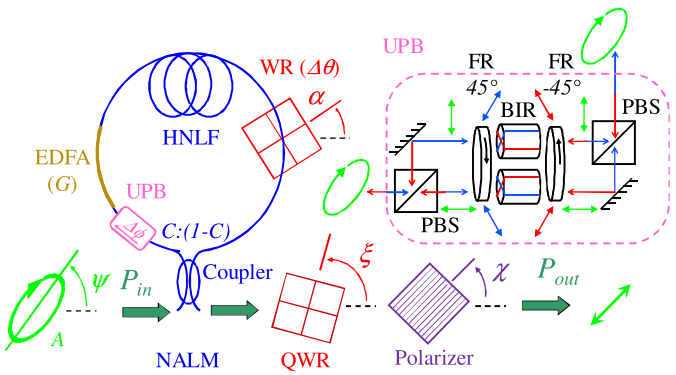

Fig. 1. Scheme of the P-NALM under study. EDFA – erbium-doped fiber amplifier, UPB – unidirectional phase bias, HNLF – high-nonlinearity fiber, (Q)WR – (quarter-)wave retarder. Dashed box: proposed UPB scheme (FR – Faraday rotator, PBS – polarizing beamsplitter, BIR – tunable birrefringent elements). Parameters $\psi = \pi/4$, $\Delta\theta = \pi/2$, $\alpha = 0$ and $\chi - \xi = -\pi/4$ are kept constant in this letter, the input Stokes parameter A being the only polarization control parameter that will be adjusted.

fiber amplifier (gain G) inserted asymmetrically in the loop. A unidirectional phase bias (UPB), introducing a phase shift $\Delta\phi$ in the clockwise (CW) direction, is also considered. Fulfilling simultaneously the conditions $C < 1-C$ and $CG \gg 1-C$ ensures that the large power imbalance as the beams counter-propagate in the HNLF (the CW beam being stronger than the counter-clockwise (CCW) beam) is inverted when they recombine at the NALM output (there, the CCW beam is stronger). Therefore, a nonlinear phase shift will be accumulated almost exclusively by the CW beam, whereas its comparatively low power at the NALM output ensures that the phase of the recombined signal will be mainly determined by the nearly linearly transmitted CCW beam. As a consequence, the power-dependent phase distortion at the NALM output is small. In addition, as in [13], the device is polarization-imbalanced due to the asymmetric insertion of a wave retarder (WR), which is practice can be conveniently implemented using a squeezer [16]. The input polarization state is strictly controlled (in a real communication channel, this condition can be met by implementing active polarization stabilization [18]), and is maintained through the coupler (and the UPB). The polarization of the CCW beam is then modified by the WR. Next, each beam propagates along the loop, conserving its ellipticity. This can be ensured in practice by twisting the fiber in the loop: twist induces optical activity and mitigates the effects of residual birefringence, so that the twisted fiber behaves as a perfectly isotropic fiber [19]. In the following, without loss of generality, we will assume that the total optical activity of the loop, β, is 0 modulo 2π; if now $\beta \neq 0$, the P-NALM operation is not altered: its transmission remains the same, provided that the WR, quarter-WR (QWR) and polarizer in Fig. 1 and the input polarization ellipse are all rotated by $\beta/2$ [14]. After the CW and CCW beams pass through the WR and amplifier respectively, they recombine at the NALM output. Finally, the P-NALM scheme is completed by inserting at the NALM output a QWR and polarizer whose purpose is to select a specific output polarization component. In summary, in addition to C, G and $\Delta\phi$, the implementation of polarization control in the P-NALM scheme introduces 6 additional adjustment parameters (angle ψ and ellipticity or Stokes parameter A of input polarization, WR retardation $\Delta\theta$ and angle α, and orientations ξ and χ of output QWR and polarizer). Although they might be dependent, this increase in the number of adjustment parameters makes the device more flexible and therefore attractive for the regeneration of complex constellations.

In this letter we illustrate the potential of the device in the frame of multilevel amplitude regeneration for a particular choice of the following parameters, which was oriented by previous studies of the polarization-imbalanced NOLM, and by numerical simulations: the WR in the loop is a QWR ($\Delta\theta = \pi/2$) with $\alpha = 0$, and the circular-left polarization component is selected at the NALM output ($\chi - \xi = -\pi/4$; in this case the orientation of the QWR+polarizer block is irrelevant). In a first step, we assume linear input polarization ($A = 0$) oriented at $\psi = \pi/4$. In practice, if $\beta \neq 0$ and is unknown, proper α and ψ settings can be found by maintaining $\psi - \alpha = \pi/4$ and maximizing the dynamic range of the NALM transmission [14]. In this case, the CW and CCW beams are linearly and circularly polarized, respectively. Assuming purely circular birefringence in the loop, and using a procedure analogous to [14] based on the Jones formalism, we find that the polarization at the NALM output is purely circular left (so that all light is transmitted through the polarizer), and the total power transmission $T = P_{out}/P_{in}$ is given by

$$T/G = 1 - 2C(1-C) \times \langle 1 + \cos\{[C(G+2/3) - 2/3]\gamma L P_{in} + \Delta\phi\}\rangle . \quad (1)$$

This result corresponds to the solid curves in Fig. 2. Equation (1) is very similar to the expression of the transmission for the NALM without polarization control, except that the switching power $P_\pi = \pi/\{[C(G+2/3) - 2/3]\gamma L\}$ is slightly reduced in comparison with the NALM without polarization control (for which $P_\pi = \pi/\{[C(G+1) - 1]\gamma L\}$), due to the polarization contribution to the imbalance. In practice however, $CG \gg 1$ and the difference is not significant. If now the input polarization is made elliptic ($A \neq 0$, while keeping the major axis at $\psi = \pi/4$), the situation is complicated, in particular both circular polarization components appear at the NALM output, and the analytic expression for T is more elaborate. For $A \ll 1$ however, polarization at the NALM output is still approximately circular left, and T can be approximated by

$$T/G \approx 1 - C^2/2\left[1 - \cos(2CGA\gamma L P_{in}/3)\right] - 2C(1-C) \times \langle 1 + \cos(CGA\gamma L P_{in}/3) \cos\{[C(G+2/3) - 2/3]\gamma L P_{in} + \Delta\phi\}\rangle . \quad (2)$$

Both the exact curves obtained through Jones matrix calculations and the approximate result from (2) are shown in Fig. 2. Apart from the $-C^2/2[1 - cos(2CGA\gamma L P_{in}/3)]$ term that appears in (2) (related to the circular right component absorbed by the polarizer, which typically amounts to a few % only), the main difference with respect to (1) is that the periodic variation of the transfer characteristic (the

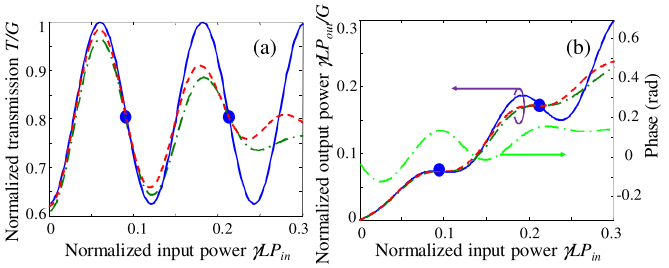

Fig. 2. (a) Transmission and (b) output power and phase characteristics of the P-NALM for linear ($A = 0$, solid blue) and elliptic ($A = 0.3138$) input polarizations (dashed-dotted green: exact solution using Jones matrix calculation, dashed red: using (2)). $G = 500$, C $= 0.1046$, $\Delta\phi = 0$, other parameters given in main text. State power ratio: 1:2.2.

third cosine in (2)) is now amplitude-modulated by a slowly-varying envelope (the second cosine). This effect is related to the nonlinear polarization rotation of the high-power CW beam, which is proportional to A. The consequence of this modulation is illustrated in Fig. 2, in which $C = 0.1046$ was chosen to have a nearly horizontal first plateau in the power transfer characteristic, $P_{out} = T \times P_{in}$. Plateaus in the P_{out} characteristic correspond to the negative slope portions of the T curve (marked by filled circles in Fig. 2). When $A = 0$ (solid curve in Fig. 2(b)), the plateaus of P_{out} beyond the first one have strong negative slopes; for $A \neq 0$ however, these can be reduced or even cancelled. Although perfect flatness cannot be obtained for all plateaus simultaneously, proper adjustments of parameters C and A allow producing two perfectly horizontal plateaus in the P_{out} characteristic (dashed-dotted curve in Fig. 2(b)). Besides, we found that this possibility persists even when A deviates substantially from 0 and (2) is no longer a valid approximation for T. Finally, the nonlinear phase shift at the P-NALM output (for $A \neq 0$) is also shown in Fig. 2(b). It appears that the values at the plateaus are small and nearly equal.

III. Application to 2-Level Amplitude Regeneration

Now we will analyze the two-level regenerative ability of the scheme for two different state power ratios. The state power ratio can be varied conveniently by tuning $\Delta\phi$. As in Fig. 2, parameters C and A are optimized to obtain two zero-slope plateau regions, as shown in Fig. 3. Other parameters are the same as in the previous section. Assuming a length $L = 100$ m of HNLF with $\gamma = 10$ W^{-1}km^{-1}, for example, the normalized values in abscissa of Fig. 3 are equal to the absolute power in W, showing that the plateau regions appear at moderate values of input power. The regenerative ability (RA), defined as the ratio between σ_{in} and σ_{out}, the standard deviations of input and output signal powers, both normalized to their average values [9], is also computed and shown in Fig. 3. For this purpose we consider a white Gaussian noise corresponding to a signal-to-noise ratio (SNR) of 18 dB when the input power matches the first plateau level, and σ_{in} is kept constant as P_{in} is varied. The high, single-peaked values of RA observed at both plateaus in each case confirm that the slopes of the plateaus cancel simultaneously for each adjustment of parameters. The figure

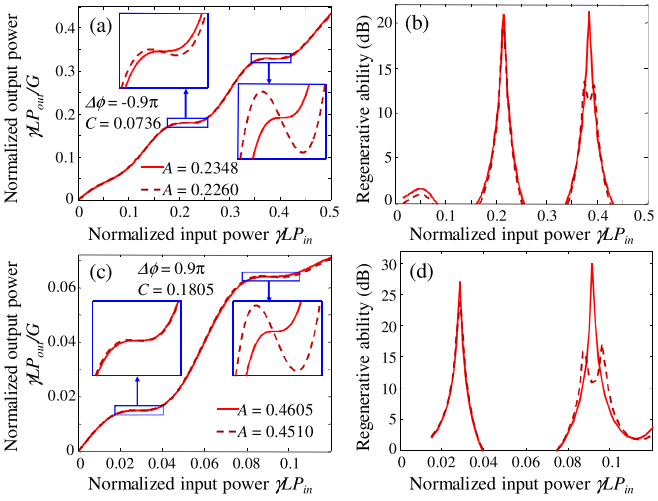

Fig. 3. (a, c) Output power characteristics and (b, d) regenerative ability of the P-NALM for two state power ratios: 1:1.8 (a, b) and 1:3.2 (c, d). Insets show expansions of the plateau regions (same vertical scale for both insets). In case (a, b), these are actually the second and third plateaus. Values of $\Delta\phi$, C and A are shown in figures; other parameters same as in section II.

also illustrates the effect of a small alteration of parameter A from its optimal value, whereas C is kept constant: the slope of the second plateau is modified, whereas the first one remains nearly flat. Consequently, the RA deteriorates at the second plateau, but remains nearly unchanged at the first plateau. If now this RA reduction is considered acceptable, this increase of A ca be viewed as a way to widen the second plateau. Similarly, varying C allows controlling the width of the first plateau, again at the price of an RA degradation. In summary, the flatness of each plateau (and its related width and RA sharpness) can be adjusted almost independently, the first one through C and the second through A. This simplifies greatly the adjustment procedure.

Finally, we demonstrate through numerical simulations the potential of the proposed scheme for cascaded regeneration along a noisy channel. We consider the star-8 quadrature amplitude modulation (QAM) format as an example. The noise is modeled as a complex white Gaussian noise uniformly distributed along the link. A variable number R of identical regenerators are inserted equidistantly along the link, dividing the channel into $R+1$ equal sections. In each section, propagation is assumed to be linear, and dispersion is neglected. In order to ensure that the state power ratio is conserved through each regenerator, in addition to A and C, $\Delta\phi$ is also optimized (independent adjustment of the power state ratio is thus no longer possible, at least by using only these three parameters). For optimal parameters $C = 0.149$, $A = 0.436$ and $\Delta\phi = 0.6\pi$, the state power ratio is 1:3.75. Hence, preservation of the state power ratio requires a constellation presenting this particular ratio. For this constellation, proper power scaling at the output of each regenerator then allows cascadability. Finally, although the phase shifts introduced by each P-NALM are small, they accumulate and can become significant for large values of R, so that an optical phase conjugator is considered in the middle of the channel. Fig. 4 shows a few illustrative results. As a reference, we take the same

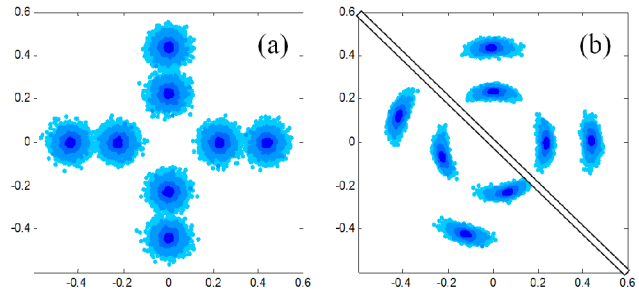

Fig. 4. Constellation diagrams of star-8QAM (a) after transmission without regeneration and (b) after 10 regenerators equidistantly placed along the link, with (upper right corner) and without (lower left corner) phase conjugator in the middle (due to symmetry, only two of the four phase states are shown in each case). The SNR of the equivalent channel without regenerator is 18 dB. P-NALM parameters: $C = 0.149$, $A = 0.436$ and $\Delta\phi = 0.6\pi$.

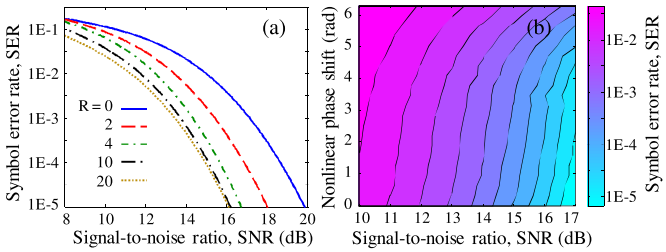

Fig. 5. (a) SER as a function of SNR, for different values of the number R of regenerators ($R = 0$: channel without regenerator). (b) Contour plot of SER as a function of SNR and nonlinear phase shift of the high power state, for $R = 10$. Results obtained with a phase conjugator in the middle of the channel.

noisy channel in the absence of the regenerators, having a SNR of 18 dB (assuming a signal of equiprobable symbols), see Fig. 4(a). Fig. 4(b) shows amplitude noise squeezing and the constellation improvement at the receiver end for $R = 10$. In order to further assess the regeneration performance, the symbol error rate (SER) is computed by direct error counting of 8×10^7 equiprobable symbols. Results are shown in Fig. 5(a) in function of the SNR of the reference channel (without regenerator), for different values of R. The figure shows that the SER improvement saturates for $R \geq 10$. In this case, performance is limited by phase noise. Further improvement would thus require the use of phase regenerators [7] in combination with the proposed amplitude regenerators. Finally, the impact of the nonlinearity of the transmission line, which introduces nonlinear phase noise, was evaluated. Fig. 5(b) presents the dependence of the SER on both the SNR and the nonlinear phase shift of the fiber span (for the high power state), for $R = 10$. The figure indicates that, for a given SNR, the SER first degrades at a slow pace as nonlinearity increases; this degradation then accelerates beyond ~4 rad.

IV. Conclusion

We proposed a flexible NALM scheme for multilevel amplitude regeneration. Its transmission characteristic relies on the control of the state of polarization. We showed that, by controlling one polarization property (namely, ellipticity at the device input) together with the coupling ratio and UPB, if all other parameters are properly set and fixed, optimal two-level amplitude regeneration for different power ratios is possible, and cascaded configurations are also feasible. Involving more than one polarization parameter in the adjustment procedure would further reveal the potential of the proposed scheme, in particular for amplitude regeneration of more complex constellations involving more than two levels. Finally, because a well-defined polarization state is used at the input and selected at the output, the scheme is compatible with polarization-multiplexing formats.

References

[1] N. J. Doran and D. Wood, "Nonlinear-optical loop mirror," *Opt. Lett.*, vol. 13, no. 1, pp. 56–58, Jan. 1988.
[2] M. E. Fermann, F. Haberl, M. Hofer, and H. Hochreiter, "Nonlinear amplifying loop mirror," *Opt. Lett.*, vol. 15, no. 13, pp. 752–754, Jul. 1990.
[3] S. Bigo, O. Leclerc, and E. Desurvire, "All-optical fiber signal processing and regeneration for soliton communications," *IEEE J. Sel. Topics Quantum Electron.*, vol. 3, no. 5, pp. 1208–1223, Oct. 1997.
[4] S. Boscolo, S. K. Turitsyn, and K. J. Blow, "Nonlinear loop mirror-based all-optical signal processing in fiber-optic communications," *Opt. Fiber Technol.*, vol. 14, no. 4, pp. 299–316, Oct. 2008.
[5] P. J. Winzer and R.-J. Essiambre, "Advanced modulation formats for high-capacity optical transport networks," *J. Lightw. Technol.*, vol. 24, no. 12, pp. 4711–4728, Dec. 2006.
[6] K. Cvecek *et al.*, "2R-regeneration of an 80-Gb/s RZ-DQPSK signal by a nonlinear amplifying loop mirror," *IEEE Photon. Technol. Lett.*, vol. 19, no. 19, pp. 1475–1477, Oct. 1, 2007.
[7] J. Kakande *et al.*, "Multilevel quantization of optical phase in a novel coherent parametric mixer architecture," *Nature Photon.*, vol. 5, no. 12, pp. 748–752, Dec. 2011.
[8] T. Roethlingshoefer, G. Onishchukov, B. Schmauss, and G. Leuchs, "All-optical simultaneous multilevel amplitude and phase regeneration," *IEEE Photon. Technol. Lett.*, vol. 26, no. 6, pp. 556–559, Mar. 15, 2014.
[9] M. Hierold, T. Roethlingshoefer, K. Sponsel, G. Onishchukov, B. Schmauss, and G. Leuchs, "Multilevel phase-preserving amplitude regeneration using a single nonlinear amplifying loop mirror," *IEEE Photon. Technol. Lett.*, vol. 23, no. 14, pp. 1007–1009, Jul. 15, 2011.
[10] M. Sorokina, "Design of multilevel amplitude regenerative system," *Opt. Lett.*, vol. 39, no. 8, pp. 2499–2502, Apr. 2014.
[11] M. A. Sorokina, S. Sygletos, and S. K. Turitsyn, "Optimization of cascaded regenerative links based on phase sensitive amplifiers," *Opt. Lett.*, vol. 38, no. 21, pp. 4378–4381, Nov. 2013.
[12] M. Sjödin, P. Johannisson, H. Wymeersch, P. A. Andrekson, and M. Karlsson, "Comparison of polarization-switched QPSK and polarization-multiplexed QPSK at 30 Gbit/s," *Opt. Exp.*, vol. 19, no. 8, pp. 7839–7846, Apr. 2011.
[13] E. A. Kuzin, N. Korneev, J. W. Haus, and B. Ibarra-Escamilla, "Theory of nonlinear loop mirrors with twisted low-birefringence fiber," *J. Opt. Soc. Amer. B*, vol. 18, no. 7, pp. 919–925, Jul. 2001.
[14] O. Pottiez, E. A. Kuzin, B. Ibarra-Escamilla, and F. Méndez-Martínez, "Theoretical investigation of the NOLM with highly twisted fibre and a $\lambda/4$ birefringence bias," *Opt. Commun.*, vol. 254, nos. 1–3, pp. 152–167, May 2005.
[15] B. Ibarra-Escamilla *et al.*, "Experimental investigation of the nonlinear optical loop mirror with twisted fiber and birefringence bias," *Opt. Exp.*, vol. 13, no. 26, pp. 10760–10767, Dec. 2005.
[16] I. Armas-Rivera *et al.*, "Experimental study of the polarization asymmetrical NOLM with adjustable switch power," *Opt. Commun.*, vol. 350, pp. 165–169, Sep. 2015.
[17] O. Pottiez, B. Ibarra-Escamilla, and E. A. Kuzin, "High-quality amplitude jitter reduction and extinction enhancement using a power-symmetric NOLM and a polarizer," *Opt. Exp.*, vol. 15, no. 5, pp. 2564–2572, Mar. 2007.
[18] R. Noé, H. Heidrich, and D. Hoffmann, "Endless polarization control systems for coherent optics," *J. Lightw. Technol.*, vol. 6, no. 7, pp. 1199–1208, Jul. 1988.
[19] T. Tanemura and K. Kikuchi, "Circular-birefringence fiber for nonlinear optical signal processing," *J. Lightw. Technol.*, vol. 24, no. 11, pp. 4108–4119, Nov. 2006.